DNA Cleavage by UVA Irradiation of NADH with Dioxygen via Radical Chain Processes

Makiko Tanaka, Kei Ohkubo, and Shunichi Fukuzumi*

Department of Material and Life Science, Graduate School of Engineering, Osaka University, SORST, Japan Science and Technology Agency, Suita, Osaka 565-0871, Japan

Received: July 1, 2006; In Final Form: July 22, 2006

Efficient DNA cleaving-activity is observed by UVA irradiation of an O_2-saturated aqueous solution of NADH (β-nicotinamide adenine dinucleotide, reduced form). No DNA cleavage has been observed without NADH under otherwise the same experimental conditions. In the presence of NADH, energy transfer from the triplet excited state of NADH (^{3}NADH*) to O_2 occurs to produce singlet oxygen ($^1O_2$) that is detected by the phosphorescence emission at 1270 nm. No quenching of $^1O_2$ by NADH was observed as indicated by no change in the intensity of phosphorescence emission of $^1O_2$ at 1270 nm in the presence of various concentrations of NADH. In addition to the energy transfer, photoinduced electron transfer from ^{3}NADH* to O_2 occurs to produce $NADH^{\bullet+}$ and $O_2^{\bullet-}$, both of which was observed by ESR. The quantum yield of the photochemical oxidation of NADH with O_2 increases linearly with increasing concentration of NADH but decreases with increasing the light intensity absorbed by NADH. Such unusual dependence of the quantum yield on concentration of NADH and the light intensity absorbed by NADH indicates that the photochemical oxidation of NADH with O_2 proceeds via radical chain processes. The $O_2^{\bullet-}$ produced in the photoinduced electron transfer is in the protonation equilibrium with $HO_2^{\bullet}$, which acts as a chain carrier for the radical chain oxidation of NADH with O_2 to produce NAD^+ and H_2O_2, leading to the DNA cleavage.

Introduction

Solar UV irradiation, particularly in the UVA region (320−400 nm), induces the formation of photoexcited states of skin photosensitizers with subsequent generation of reactive oxygen species (ROS) and other toxic photoproducts, being a major risk factor in the development of skin cancer.[1−5] UVA radiation constitutes >90% of the environmentally relevant solar UV radiation, because UVC (190−280 nm) and short-wavelength UVB (280−295 nm) are mostly blocked by the atmosphere.[6] At present, however, the premutagenic DNA lesions induced by UVA have not been identified.

NADH (nicotinamide adenine dinucleotide), a naturally occurring coenzyme found in all living cells, has an absorption maximum around 340 nm and thereby absorbs UVA light. Thus, NADH may be regarded a potential photosensitizer to generate ROS. Indeed the induction of breaks in DNA in vitro caused by 334 nm UV radiation has been reported to be enhanced by the presence of NADH via formation of $O_2^{\bullet-}$.[7−9] This indicate that an endogenous compound such as NADH may participate in the production of $O_2^{\bullet-}$ by solar UVA irradiation and imply that $O_2^{\bullet-}$ may play a role in sunlight-induced erythema and dermal carcinogenesis. Superoxide ion is also produced by photosensitization with fullerene derivatives in the presence of NADH.[10,11] However, the detailed mechanism of $O_2^{\bullet-}$ generation in UVA irradiation of NADH with dioxygen and the relation with the DNA cleavage have yet to be clarified. The possible intermediacy of $^1O_2$ that may be produced by photosentization of NADH should also be clarified, because it is proposed that $^1O_2$ reacting with guanosine or deoxyguanosine part of nucleotides does not, by itself, cause DNA cleavage.[12]

We report herein detailed spectroscopic and kinetic studies on UVA-induced DNA cleavage by the photochemical reaction of NADH with O_2, detection of superoxide ($O_2^{\bullet-}$) by ESR as well as detection of $^1O_2$ phosphorescence to provide confirmative mechanistic insight into the photoinduced DNA damage by NADH with O_2.

Experimental Section

Materials. NADH (β-nicotinamide adenine dinucleotide, reduced form), catalase and $FeSO_4$ were purchased from Sigma Chemical Co. DNA pBR322 (0.32 μg μL^{-1}) and superoxide dismutase (SOD) were purchased from Wako Pure Chemical Ind. Ltd., Japan. Dimethyl sulfoxide (DMSO) and methanol were purchased from Nacalai Tesque Co., Ltd. Potassium ferrioxalate used as an actinometer was prepared according to the literature and purified by recrystallization from hot water.[13] Purification of water (18.3 MW cm) was performed with a Milli-Q system (Millipore; Milli-Q Jr.).

DNA Cleavage. Typically, 18 μL of aqueous buffer solution of NADH (2.1×10^{-2} M) and 2 μL of aqueous solution of DNA pBR322 (0.32 μg μL^{-1}) were mixed in a micro test tube under dark conditions. Samples were incubated under irradiation with a monochromatized light ($\lambda = 340$ nm) from a Shimadzu RF-5300PC spectrophotometer at 298 K. The 2 μL of aqueous solution of DNA pBR322 (0.032 μg μL^{-1}) was diluted by adding 18 μL of water, then mixed with 2 μL of loading buffer (0.1% bromophenol blue and 3.75% Ficol in TAE buffer) and loaded onto 1.4% agarose gel. The gel was run at a constant voltage of 130 V for 50 min in TAE buffer using a Nihon Eido electrophoresis kit, then washed with distilled water, soaked into 0.1% ethidium bromide aqueous solution, visualized under a UV transilluminator, and photographed using a digital camera.

ESR Measurements. In a typical experiment of the ESR measurements for the detection of O_2, 0.5 mL of an aqueous buffer solution (50 mM Tris/HCl (pH 7.0)) of NADH (1.4 M) was saturated with O_2 in an ESR sample tube (internal diameter: 4 mm). The ESR sample was then irradiated with a 1000-W high-pressure mercury lamp (Ushio-USH1005D) through an aqueous filter at 298 K and immediately measured at 123 K. ESR spectra were measured with a JEOL JES-ME-LX and were recorded under nonsaturating microwave power conditions. The magnitude of the modulation was chosen to optimize the

* Corresponding author. E-mail: fukuzumi@chem.eng.osaka-u.ac.jp.

10.1021/jp064130r CCC: $33.50
Published on Web 08/26/2006

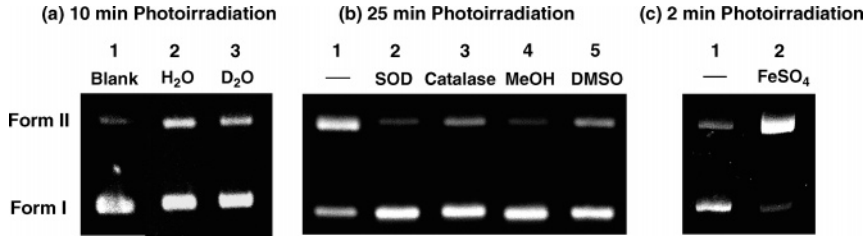

Figure 1. Agarose gel electrophoresis of cleavage of supercoiled pBR322 DNA (7.4×10^{-6} M) in the reaction of photoirradiated NADH (1.9×10^{-2} M) with O_2 in air-saturated aqueous buffer solution (pH 5.5) at 298 K. (a) Cleavage of DNA after 10 min photoirradiation of monochromatized light ($\lambda = 340$ nm). Lane 1, blank; lane 2, in H_2O; lane 3, in D_2O. (b) Cleavage of DNA after 25 min photoirradiation of monochromatized light ($\lambda = 340$ nm). Lane 1, no scavenger and inhibitor; lane 2, + 100 μg mL^{-1} SOD; lane 3, + 40 μg mL^{-1} catalase; lane 4, + 10% methanol; lane 5, + 10% DMSO. (b) Cleavage of DNA after 2 min photoirradiation of monochromatized light. Lane 1, in the absence of $FeSO_4$; lane 2, in the presence of $FeSO_4$ (6.4×10^{-4} M).

resolution and the signal-to-noise ratio (S/N) of the observed spectra. The *g* values were calibrated using an Mn^{2+} marker.

Spectroscopic Measurements. Typically, an air-saturated 50 mM Tris/HCl buffer solution (pH 7.0; 3 mL) of NADH (4.8×10^{-2} to 2.5×10^{-1} M) in a quartz cuvette (10 mm i.d.) under an atmospheric pressure was irradiated with a xenon lamp (Ushio model V1-501C) through a UV cut-off filter transmitting $\lambda > 310$ nm at 298 K for 110 min. The concentration of absorbed photons by NADH was changed by using quartz cuvettes with different path lengths (10 mm, 2 mm, and 1 mm). The UV−vis spectra were measured on a Shimadzu UV-3100PC spectrophotometer. The amount of H_2O_2 produced in the photochemical reaction of NADH with O_2 was determined by titration with iodide ion.[14] For the singlet oxygen emission measurements, an O_2-saturated D_2O solution containing NADH ($5.8 \times 10^{-5} - 1.6 \times 10^{-3}$ M) in a quartz cell (optical path length 10 mm) was excited at $\lambda = 340$, 372, and 384 nm using a Cosmo System LVU-200S spectrometer. Near-IR emission spectra of singlet oxygen were measured on a SPEX Fluorolog τ3 fluorescence spectrophotometer. A photomultiplier (Hamamatsu Photonics, R5509−72) was used to detect emission in the near-infrared region.

Quantum Yield Determination. A standard actinometer (potassium ferrioxalate)[13] was used for the quantum yield determination of the photochemical reactions of NADH. A square quartz cuvette which contained a 50 mM Tris/HCl buffer solution (pH 7.0; 3 mL) of NADH (9.9×10^{-3} M) was irradiated with monochromatized light of $\lambda = 340$ nm from a Shimadzu RF-5300PC fluorescence spectrophotometer. Under the conditions of actinometry experiments, both the actinometer and NADH absorbed essentially all the incident light. The light intensity of monochromatized light of $\lambda = 340$ nm was determined as 1.7×10^{-8} einstein s^{-1}. The photochemical reaction was monitored using a Shimadzu UV-3100PC spectrophotometer. The quantum yields were determined from the decrease from the absorbance due to NADH ($\lambda = 340$ nm, $\epsilon = 6.0 \times 10^3$ M^{-1} cm^{-1}).

Results and Discussion

Photoinduced DNA Cleavage in the Aqueous NADH−O_2 System. There are two possible pathways of generation of active species responsible for DNA cleavage in the NADH−O_2 system under UVA irradiation (Scheme 1). One is photoinduced electron transfer from NADH to O_2 to produce $O_2^{\bullet-}$ (type I) and the other is energy transfer from NADH to O_2 to produce $^1O_2$ (type II).[11] In both pathways the triplet excited state (^{3}NADH*) formed by intersystem crossing from the singlet excited state (^{1}NADH*) is involved. To clarify the active species mainly responsible for the DNA cleavage activity upon UVA irradiation of NADH with O_2, the widely used assay with pBR322 supercoiled DNA[15] was employed (vide infra).

SCHEME 1: Two Possible Pathways of Generation of Active Species in the NADH−O_2 System under UVA Irradiation

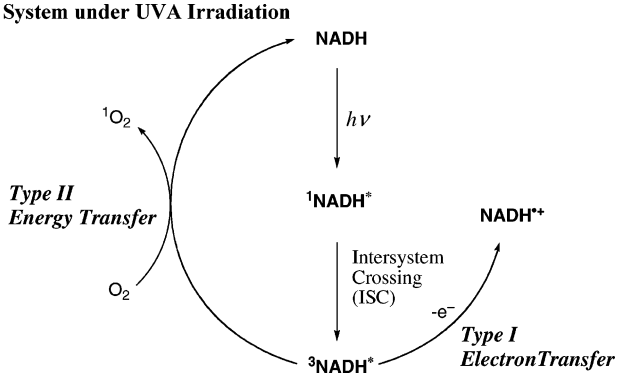

The supercoilded DNA (form I) is efficiently cleaved into form II (nicked DNA) by 10 min UVA-light irradiation of an air-saturated CH_3COOH/KOH buffer solution (10 mM, pH 5.5) of NADH with use of a monochromatized light ($\lambda = 340$ nm) from a xenon lamp as shown in Figure 1a (lane 2). Under dark conditions, no DNA cleavage occurs in the presence of all the components, i.e., NADH, and O_2. To test the possible role of $^1O_2$, the effect of $^1O_2$ stabilizer was tested. When H_2O is replaced by D_2O, which is known to prolong the lifetime of $^1O_2$,[16] the DNA cleavage activity was not affected at all (lane 3 in Figure 1a). This indicates that $^1O_2$, which was previously reported to be important for the photoinduced bioactivities,[17,18] does not play a significant role in the DNA-cleaving activity in the NADH−O_2 system under UVA irradiation. In contrast, the effect of the $^1O_2$ stabilizer, the DNA cleaving activity was clearly inhibited by the addition of superoxide dismutase (SOD),[19] which quenches $O_2^{\bullet-}$ (lane 2 in Figure 1b). This suggests that formation of $O_2^{\bullet-}$ plays an essential role in the DNA cleavage. However, this does not necessarily mean that $O_2^{\bullet-}$ is an actual reactive species for the DNA cleavage, since $O_2^{\bullet-}$ is generally regarded as a rather unreactive radical species.[20]

Addition of an H_2O_2-destroying enzyme catalase significantly inhibits DNA cleavage (lane 3 in Figure 1b). Addition of hydroxyl radical scavengers such as methanol (lane 4) and DMSO (lane 5) also inhibits DNA cleavage. Thus, the actual reactive species for the DNA cleavage may be hydroxyl radical produced in a reaction between NAD$^\bullet$ and H_2O_2.[21] The addition of $FeSO_4$ to the NADH−O_2 system after UVA irradiation enhances the DNA cleavage reactivity significantly by the effective formation of hydroxyl radical in the Fenton reaction[22] (lane 2 in Figure 1c).

The pH dependence of the DNA cleavage reactivity was examined as shown in Figure 2. The DNA cleavage reactivity increases with decreasing pH. The DNA was cleaved into form

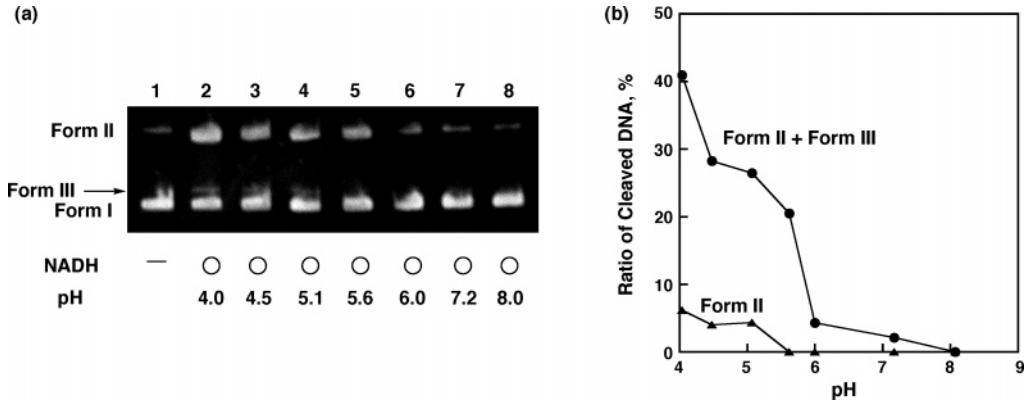

Figure 2. (a) Agarose gel electrophoresis of cleavage of supercoiled pBR322 DNA (7.3×10^{-6} M) in the reaction of photoirradiated NADH (1.9×10^{-2} M) with O_2 in air-saturated 10 mM aqueous buffer solution (pH 4.0−8.0) at 298 K after 16 min photoirradiation of monochromatized light ($\lambda = 340$ nm). (b) pH profiles of photoinduced cleavage ratio of supercoiled pBR322 DNA.

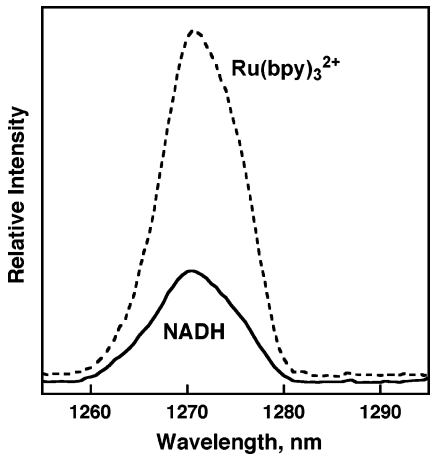

Figure 3. Near-infrared singlet oxygen luminescence emission spectra in NADH (1.5×10^{-4} M) and $Ru(bpy)_3^{2+}$ (1.6×10^{-4} M) as reference with excitation at 340 nm in D_2O. The absorbance of NADH and $Ru(bpy)_3^{2+}$ at 340 nm is adjusted to be the same as 0.90.

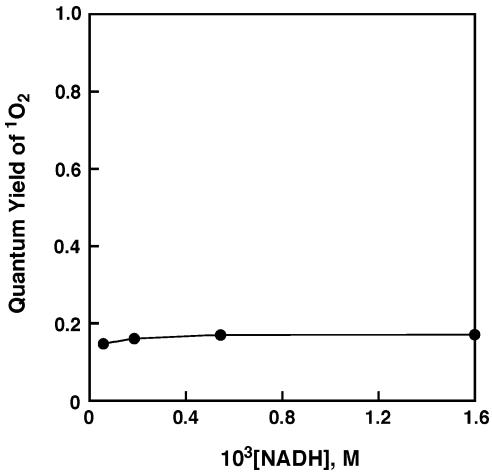

Figure 4. Quantum yield of $^1O_2$ formation in the presence of various concentrations of NADH ($5.7 \times 10^{-5} - 1.6 \times 10^{-3}$ M) in an O_2-saturated D_2O solution.

II and form III (linear DNA). The enhanced DNA cleavage reactivity at low pH may result from the protonation of $O_2^{\bullet-}$ to produce $HO_2^{\bullet}$ ($pK_a = 4.9$).[23,24]

Photoinduced Generation of $O_2^{\bullet-}$ with NADH. Photoexcitation of NADH in a neutral aqueous solution results in fluorescence emission at 460 nm. This was scarcely been quenched by O_2 due to the short lifetime (0.4 ns).[25,26] The singlet excited state of NADH is known to be efficiently converted to the triplet excited state (^{3}NADH*) by the fast intersystem crossing.[25] The phosphorescence spectrum of NADH has been reported previously.[27] The excited-state energy of ^{3}NADH* is evaluated as 2.9 eV from the phosphorescence maximum. In the presence of O_2, energy transfer from ^{3}NADH* to O_2 affords $^1O_2$ (type II in Scheme 1). The phosphorescence of $^1O_2$ is observed at 1270 nm by the photoexcitation of an O_2-saturated D_2O solution of NADH as shown in Figure 3, where $^1O_2$ formation by the photoexcitation of $Ru(bpy)_3^{2+}$ is also shown for comparison.[28] The quantum yield of $^1O_2$ formation by the photoexcitation of an O_2-saturated D_2O solution of NADH is determined as 0.16.

Singlet oxygen ($^1O_2$: $^1\Delta_g$) produced in an energy transfer from ^{3}NADH* to O_2 in Scheme 1 was suggested to be reduced by NADH to $O_2^{\bullet-}$.[29] In general, $^1O_2$ is quenched by physical and chemical processes in which only the latter gives the actual products.[30,31] In the present case, however, no quenching of $^1O_2$ by NADH is observed, because the quantum yield of $^1O_2$ formation remains constant when concentration of NADH is increased up to 1.6×10^{-3} M (Figure 4). This is consistent with the energetics of electron transfer from NADH to $^1O_2$. The one-electron reduction potential of $^1O_2$ in water is evaluated as ($E_{red}^* = 0.58$ V) by adding the excitation energy of $^1O_2$ (0.98 eV)[30] to the E_{red} value of O_2 in H_2O (−0.40 V).[23] Since the one-electron oxidation potential of NADH ($E_{ox} = 0.69$ V)[32,33] is higher than the E_{red} value of $^1O_2$, the electron transfer from NADH to $^1O_2$ is thermodynamically not feasible.[34] In contrast, electron transfer from ^{3}NADH* to O_2 highly exergonic, because the E_{ox} value of ^{3}NADH* (−2.2 V vs SCE)[35] is much more negative than the E_{red} value of O_2 (−0.40 V vs SCE).[23] Thus, $NADH^{\bullet+}$ and $O_2^{\bullet-}$ may be formed via direct electron transfer from ^{3}NADH* to O_2 rather than electron transfer from the ground-state NADH to $^1O_2$.

Formation of $NADH^{\bullet+}$ and $O_2^{\bullet-}$ upon photoexcitation of NADH with O_2 is confirmed by the ESR spectrum measured at 173 K as shown in Figure 5. The anisotropic signal at $g_{\parallel} = 2.13$ and $g_{\perp} = 2.003$ (Figure 5a) is assigned to $O_2^{\bullet-}$.[36,37] The isotropic ESR signal due to $NADH^{\bullet+}$ may be overlapped at $g = 2.003$.[38] The ESR signal is also observed at $g = 4.0$ due to the $\Delta M_S = 2$ transition (Figure 5b). The observation of a "$\Delta M_S = 2$" line in the region of $g = 4.0$ is the diagnostic marker for detection of the triplet state.[39] The zero-field splitting parameters D and E are determined from the randomly oriented triplet system. The separation of the outer vertical lines corresponds to $2|D|$, whereas that of the intermediated and inner pairs is $|D| + 3|E|$ and $|D| - 3|E|$, respectively. The triplet signal is attributed to the radical ion pair ($NADH^{\bullet+}$ and $O_2^{\bullet-}$). Since D depends on the distance between two electrons with parallel

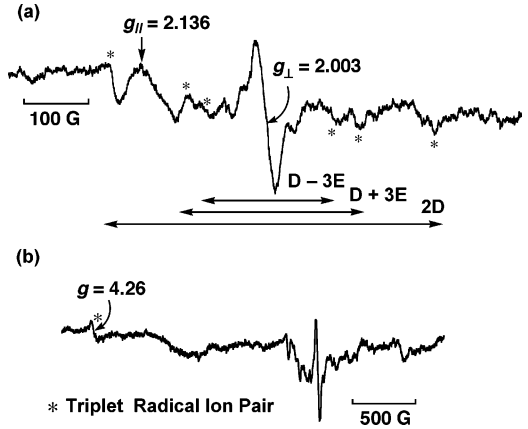

Figure 5. (a) ESR spectrum of $O_2^{\bullet-}$ generated in the photoinduced electron transfer from NADH to O_2 in O_2-saturated NADH (1.4 M) aqueous buffer solution (pH 7.0) under photoirradiation with a high pressure mercury lamp at 298 K and immediately measured at 123 K. Asterisks show signals assigned to triplet radical ion pair. (b) ESR signal ($g = 4.26$) assigned to the triplet radical ion pair.

spins, the average distance of two spins can be evaluated from the D values.[39] The distance between two electrons (R) for the radical ion pair is determined as 4.8 Å.

Radical Chain Mechanism of Photoinduced Reduction of O_2 by NADH. The overall stoichiometry of the photochemical reaction of NADH with O_2 is given by eq 1.

$$\mathrm{NADH} + \mathrm{O_2} + \mathrm{H^+} \xrightarrow[h\nu]{} \mathrm{NAD^+} + \mathrm{H_2O_2} \qquad (1)$$

NADH is a two-electron reductant that can reduce O_2 to H_2O_2 to afford NAD^+.[40] The formation of NAD^+ was confirmed by the ^{1}H NMR spectrum. After the completion of the photochemical reaction, an approximately equivalent amount of H_2O_2 was formed (see Experimental Section).

The quantum yield (Φ) for the photochemical reaction of NADH with O_2 was determined from the disappearance of the absorption band at 340 nm (see Experimental Section). In the presence of NADH (9.9×10^{-3} M), the Φ value was determined as 2.5×10^{-2} by monochromatized light (340 nm) irradiation. The dependence of the Φ value on the NADH concentration and light intensity was examined using a xenon lamp when the relative rates have been determined more accurately. The total light intensity with a xenon lamp absorbed by NADH remains nearly the same under the present experimental conditions.[41] The disappearance of the absorption band of NADH was measured under pH 7.0, because NADH slowly decomposes under lower pH (<7).[24] The Φ value increases linearly with increasing concentration of NADH with an intercept (0.0096 $\pm$ 0.0031) as shown in Figure 6.[42] The Φ value is normally independent of concentration of photons absorbed by the photoactive species. In the present case, however, the Φ value decreases with increasing concentration of photons absorbed by NADH as shown in Figure 7. In such a case, photoinduced radical chain processes are involved as shown in Scheme 2.

In the initiation step, the photoexcitation of NADH results in the formation of ^{1}NADH*, followed by intersystem crossing to produce ^{3}NADH*. Then electron transfer from ^{3}NADH* to O_2 occurs to form $NADH^{\bullet+}$ and $O_2^{\bullet-}$. The produced $O_2^{\bullet-}$ is in protonation equilibrium with $HO_2^{\bullet}$ that can abstract hydrogen from NADH to produce $NAD^{\bullet}$ and H_2O_2.[41] The electron transfer from $NAD^{\bullet}$ to O_2 reproduces $O_2^{\bullet-}$,[41] constituting a chain propagation step. The termination step is the disproportionation of $HO_2^{\bullet}$ to yield H_2O_2 and O_2 (Scheme 2).

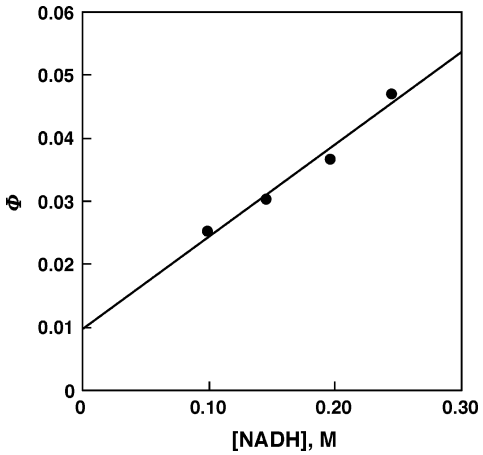

Figure 6. Dependence of the quantum yield (Φ) on NADH concentration for the photooxidation of NADH by dioxygen in an aqueous buffer solution (pH 7.0) (light: $\lambda_{ex} > 310$ nm).

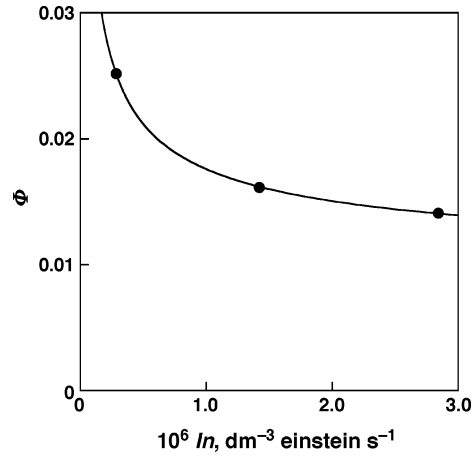

Figure 7. Dependence of the quantum yield (Φ) on the light intensity (In) for the photooxidation of NADH by dioxygen in an aqueous buffer solution (pH 7.0) (light: $\lambda_{ex} > 310$ nm).

SCHEME 2: Photoinduced Radical Chain Process of NADH

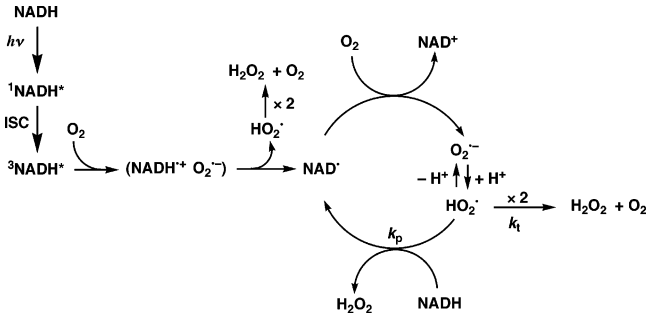

According to Scheme 2, the rate of disappearance of NADH is given by eq 2, where Φ_0 is the quantum yield of the initiation step, In is the light intensity absorbed by NADH, and k_p is the rate constant of the rate-determining propagation step (hydrogen

$$-\mathrm{d[NADH]}/\mathrm{d}t = \Phi_0 In + k_p[\mathrm{NADH}][\mathrm{HO_2^{\bullet}}] \qquad (2)$$

abstraction of $HO_2^{\bullet}$ from NADH). By applying the steady-state approximation to the radical species ($HO_2^{\bullet}$ and $NAD^{\bullet}$) in Scheme 2, concentration of $HO_2^{\bullet}$ is given by eq 3,

$$[\mathrm{HO_2^{\bullet}}] = (\Phi_0 In/k_t)^{1/2} \qquad (3)$$

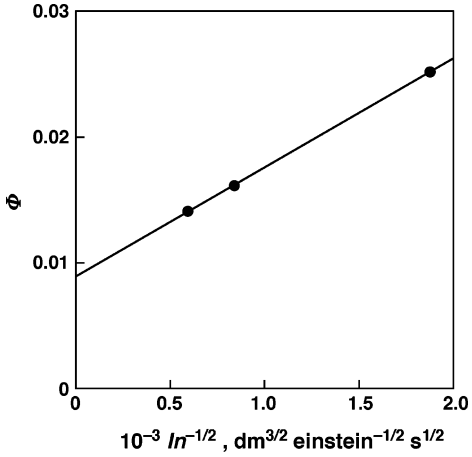

Figure 8. Plot of Φ vs $In^{-1/2}$ for the photooxidation of NADH by dioxygen in an aqueous buffer solution (pH 7.0) (light: $\lambda_{ex} > 310$ nm). The data in Figure 7 are replotted.

where k_t is the rate constant of the termination step. Then the quantum yield [$\Phi = (-d[NADH]/dt)/In$] is given as the function of the light intensity (In) and concentration of NADH (eq 4). Equation 4 agrees with the experimental results: the Φ value

$$\Phi = \Phi_0 + k_p(\Phi_0/k_t In)^{1/2}[NADH] \qquad (4)$$

increases linearly with increasing concentration of NADH with an intercept (Figure 6) and a plot of Φ vs $In^{-1/2}$ affords a linear correlation with an intercept (Figure 8). The intercept in Figure 8 agrees with that in Figure 6, corresponding to the Φ_0 value (0.0089 ± 0.0010).

In conclusion, the UVA irradiation of NADH with O_2 results in formation of $O_2^{\bullet-}$ efficiently via electron transfer (Scheme 3). The $HO_2^{\bullet}$, which is in protonation equilibrium with $O_2^{\bullet-}$, acts as a chain carrier for the radical chain processes in photochemical reaction of NADH with O_2, leading to the DNA cleavage.

Acknowledgment. This work was partially supported by a Grant in Aid (Nos. 17750039 and 16205020) from the Ministry of Education, Culture, Sports, Science, and Technology, Japan.

References and Notes

(1) Kozmin, S.; Slezak, G.; Reynaud-Angelin, A.; Elie, C.; de Rycke, Y.; Boiteux, S.; Sage, E. *Proc. Natl. Acad. Sci. U.S.A.* **2005**, *102*, 13538.

(2) Cadet, J.; Courdavault, S.; Ravanat, J.-L.; Douki, T. *Pure Appl. Chem.* **2005**, *77*, 947.

(3) Wondrak, G. T.; Roberts, M. J.; Jacobson, M. K.; Jacobson, E. L. *J. Biol. Chem.* **2004**, *279*, 30009.

(4) Wondrak, G. T.; Jacobson, M. K.; Jacobson, E. L. *Photochem. Photobiol. Sci.* **2006**, *5*, 215.

(5) Besaratinia, A.; Synold, T. W.; Chen, H.-H.; Chang, C.; Xi, B.; Riggs, A. D.; Pfeifer, G. P. *Proc. Natl. Acad. Sci. U.S.A.* **2005**, *102*, 10058.

(6) Gasparro, F. P. *Environ. Health Perspect.* **2000**, *108*, 71.

(7) (a) Peak, J. G.; Peak, M. J.; MacCoss, M. *Photochem. Photobiol.* **1984**, *39*, 713. (b) Cunningham, M. L.; Johnson, J. S.; Giovanazzi, S. M.; Peak, M. J. *Photochem. Photobiol.* **1985**, *42*, 125.

(8) Hiraku, Y.; Ito, K.; Kawanishi, S. *Photomed. Photobiol.* **2003**, *25*, 29.

(9) Cunningham, M. L.; Krinsky, N. I.; Giovanazzi, S. M.; Peak, M. J. *J. Free Radic. Biol. Med.* **1985**, *1*, 381.

(10) Yamakoshi, Y.; Umezawa, N.; Ryu, A.; Arakane, K.; Miyata, N.; Goda, Y.; Masumizu, T.; Nagano, T. *J. Am. Chem. Soc.* **2003**, *125*, 12803.

(11) (a) Nakanishi, I.; Fukuzumi, S.; Konishi, T.; Ohkubo, K.; Fujitsuka, M.; Ito, O.; Miyata, N. *J. Phys. Chem. B* **2002**, *106*, 2372. (b) Nakanishi, I.; Ohkubo, K.; Fujita, S.; Fukuzumi, S.; Konishi, T.; Fujitsuka, M.; Ito, O.; Miyata, N. *J. Chem. Soc., Perkin Trans. 2* **2002**, 1829.

(12) Chanon, M.; Julliard, M.; Mehta, G.; Maiya, B. G. *Res. Chem. Intermed.* **1999**, *25*, 633.

(13) (a) Hatchard, C. G.; Parker, C. A. *Proc. R. Soc. London, Ser. A* **1956**, *235*, 518. (b) Calvert, J. G.; Pitts, J. N. In *Photochemistry*; Wiley: New York, 1966; p 783.

(14) Fukuzumi, S.; Kuroda, S.; Tanaka, T. *J. Am. Chem. Soc.* **1985**, *107*, 3020.

(15) (a) Yamakoshi, Y.; Sueyoshi, S.; Fukuhara, K.; Miyata, N.; Masumizu, T.; Kohno, M. *J. Am. Chem. Soc.* **1998**, *120*, 12363. (b) Fukuzumi, S.; Yukimoto, K.; Ohkubo, K. *J. Am. Chem. Soc.* **2004**, *126*, 12794.

(16) Foote, C. S. *Top. Curr. Chem.* **1994**, *169*, 347.

(17) Chiang, L. Y.; Lu, F.-J.; Lin, J.-T. *J. Chem. Soc., Chem. Commun.* **1995**, 1283. (b) Lai, Y.-L.; Chiou, W.-Y.; Chiang, L. Y. *Fullerene Sci. Technol.* **1997**, *5*, 1057.

(18) (a) Tokuyama, H.; Yamago, S.; Nakamura, E.; Shiraki, T.; Sugiura, Y. *J. Am. Chem. Soc.* **1993**, *115*, 7918. (b) Boutorine, A. S.; Tokuyama, H.; Takasugi, M.; Isobe, H.; Nakamura, E.; Hélène, C. *Angew. Chem., Int. Ed. Engl.* **1994**, *33*, 2462. (c) Irie, K.; Nakamura, Y.; Ohigashi, H.; Tokuyama, H.; Yamago, S.; Nakamura, E. *Biosci., Biotechnol., Biochem.* **1996**, *60*, 1359. (d) Nakamura, E.; Tokuyama, H.; Yamago, S.; Shiraki, T.; Sugiura, Y. *Bull. Chem. Soc. Jpn.* **1996**, *69*, 2143.

(19) (a) Eliot, H.; Gianni, L.; Myers, C. *Biochemistry* **1984**, *23*, 928. (b) Nagai, K.; Hecht, S. M. *J. Biol. Chem.* **1991**, *266*, 23994. (c) Parraga, A.; Orozco, M.; Portugal, J. *Eur. J. Biochem.* **1992**, *208*, 227.

(20) Sawyer, D. T.; Valentine, J. S. *Acc. Chem. Res.* **1981**, *14*, 393.

(21) The DNA cleavage may result from OH radicals, which are formed by electron transfer from $NAD^{\bullet}$ to H_2O_2 rather than by a trace-metal Fenton reaction of H_2O_2, because the results of DNA cleavage using purified water were reproducible.

(22) Sigman, D. S.; Mazumder, A.; Perrin, D. M. *Chem. Rev.* **1993**, *93*, 2295.

(23) Sawyer, D. T.; Roberts, J. L., Jr. *Acc. Chem. Res.* **1988**, *21*, 469.

(24) The DNA cleavage reactivity could not be examined at lower pH because NADH decomposes due to acid-catalyzed hydration; see: (a) Johnston, C. C.; Gardner, J. L.; Suelter, C. H.; Metzler, D. E. *Biochemistry* **1963**, *2*, 689. (b) van Eikeren, P.; Grier, D. L.; Eliason, J. *J. Am. Chem. Soc.* **1979**, *101*, 7406.

(25) Fukuzumi, S.; Tanaka, T. In *Photoinduced Electron Transfer*; Fox, M. A.; Chanon, M., Eds.; Elsevier: Amsterdam; 1988; Part C; Chapter 10.

(26) Blinova, K.; Carroll, S.; Bose, S.; Smirnov, A. V.; Harvey, J. J.; Knutson, J. R.; Balaban, R. *Biochemistry* **2005**, *44*, 2585.

(27) Ross, J. B. A.; Rousslang, K. W.; Motten, A. G.; Kwiram, A. L. *Biochemistry* **1979**, *18*, 1808.

(28) Mulazzani, Q. G.; Sun, H.; Hoffman, M. Z.; Ford, W. E.; Rodgers, M. A. J. *J. Phys. Chem.* **1994**, *98*, 1145.

(29) (a) Peters, G.; Rodgers, M. A. J. *Biochem. Bipophys. Res. Commun.* **1980**, *96*, 770. (b) Peters, G.; Rodgers, M. A. J. *Biochim. Biophys. Acta, Bionergetics* **1981**, *637*, 43.

(30) (a) Foote, C. S. *Acc. Chem. Res.* **1968**, *1*, 104. (b) Kearns, D. R. *Chem. Rev.* **1971**, *71*, 395. (c) Stephenson, L. M.; Grdina, M. J.; Orfanopoulos, M. *Acc. Chem. Res.* **1980**, *13*, 419. (d) Foote, C. S.; Clennan, E. L. In *Properties and Reactions of Singlet Oxygen. In Active Oxygen in Chemistry*; Foote, C. S., Valentine, J. S., Greenberg, A., Liebman, J. F., Eds.; Chapman and Hall: London, 1995; pp 105−140.

(31) Wilkinson, F.; Helman, W. P.; Ross, A. B. *J. Phys. Chem. Ref. Data* **1995**, *24*, 663.

(32) Carlson, B. W.; Miller, L. L.; Neta, P.; Grodkowski, J. *J. Am. Chem. Soc.* **1984**, *106*, 7233.

(33) Zhu, X.-Q.; Yang, Y.; Zhang, M.; Cheng, J.-P. *J. Am. Chem. Soc.* **2003**, *125*, 15298.

(34) For electron-transfer reactions of $^1O_2$, see: Fukuzumi, S.; Fujita, S.; Suenobu, T.; Yamada, H.; Imahori, H.; Araki, Y.; Ito, O. *J. Phys. Chem. A* **2002**, *106*, 1241.

(35) The one-electron oxidation potential of ^{3}NADH* in water is evaluated as ($E_{ox}^* = -2.2$ V vs SCE) by subtracting the excitation energy of ^{3}NADH* (2.9 eV) from the E_{ox} value of NADH in H_2O (0.69 V vs SCE).[32,33]

(36) Bagchi, R. N.; Bond, A. M.; Scholz, F.; Stösser, R. *J. Am. Chem. Soc.* **1989**, *111*, 8270.

(37) Fukuzumi, S.; Patz, M.; Suenobu, T.; Kuwahara, Y.; Itoh, S. *J. Am. Chem. Soc.* **1999**, *121*, 1605.

(38) Fukuzumi, S.; Inada, O.; Suenobu, T. *J. Am. Chem. Soc.* **2003**, *125*, 4808.

(39) Wertz, J. E.; Bolton, J. R. *Electron Spin Resonance, Elementary Theory and Practival Applications*; McGraw-Hill: New York, 1972.

(40) Vitinius, U.; Schaffner, K.; Demuth, M.; Heibel, M.; Selbach, H. *Chem. Biodiv.* **2004**, *1*, 1487.

(41) Fukuzumi, S.; Ishikawa, M.; Tanaka, T. *J. Chem. Soc., Perkin Trans. 2* **1989**, 1037.

(42) The experimental error is within 10%.

(43) Since electron transfer from ^{3}NADH* to O_2 is highly exergonic, the electron transfer may be more favorable as compared with the H atom abstraction by O_2 from ^{3}NADH*.